

Optimization Power System Stabilizer and Energy Storage Using Ant Colony Optimization

Muhammad Ruswandi Djalal
Department of Mechanical Engineering
State Polytechnic of Ujung Pandang
wandi@poliupg.ac.id

Makmur Saini
Department of Mechanical Engineering
State Polytechnic of Ujung Pandang
makmur.saini@poliupg.ac.id

A.M. Shiddiq Yunus
Department of Mechanical Engineering
State Polytechnic of Ujung Pandang
shiddiq@poliupg.ac.id

Abstract—A sudden and severe load change may result in dynamic stability issues and adverse effects to the generator performance because of the frequency and rotor angle oscillations. Power system stabilizer (PSS) is usually used to overcome this issue however, it may fail to suppress large dynamic oscillations. This paper presents a complimentary suppression scheme using superconducting magnetic energy storage (SMES) and capacitor energy Storage (CES) systems. SMES has a rapid response to any disturbance while the CES features large storage capacity. Combination of SMES and CES can improve the performance of power systems significantly, if their control parameters are properly optimized. Traditionally, the control parameters of SMES and CES are adjusted by trial and error approach which is time consuming and does not warrant optimum performance. In this paper, ant colony optimization technique is used to simultaneously tune the SMES-CES-PSS parameters. The proposed system along with the optimized parameters is tested on a single machine-infinite bus system to assess its robustness to improve the frequency response and rotor angle profiles under severe load dynamic change. Simulation results reveal the effectiveness of the proposed controller in suppressing large oscillations and improving system stability during such disturbance events. From the optimization process, the minimum fitness function value is $6.183e-08$ at the 30th iteration.

Keywords—optimization, stability, energy storage, power system stabilizer, ant colony optimization.

I. INTRODUCTION

In studies of power system dynamic stability, governor response to torque variation is very slow when compared to the excitation system response and can be neglected. Therefore, the excitation system plays a key role in stabilizing power systems under load dynamic changes. However, the excitation amplifier circuit is less effective in stabilizing low frequency oscillations in the range 0.2 - 2.0 Hz [1].

Low frequencies can lead to oscillations on the tie-lines connecting two areas, therefore the installation of a supplementary control scheme such as power system stabilizer (PSS) is essential. PSS is an additional control system used to provide additional damping for generator excitation [2]. In addition, it can reduce the local and global oscillations in the power system. However, it may fail to suppress large dynamic oscillations within particular frequency range [3, 4]. Superconducting magnetic energy Storage (SMES) is a device used for storing and releasing large amount of energy based on the requirement of the power system it is connected to. On the other hand, capacitive energy storage (CES) is another technology that finds several applications in modern power systems. The combination of the above-mentioned

technologies features the advantage of rapid response of the SMES at reduced storage capacity and hence cost and large storage capacity of the CES. To achieve optimum performance of such combination, it is necessary to tune the PSS, SMES and CES parameters precisely [5-7]. In this paper, simultaneous tuning of these parameters is conducted using the ant colony optimization (ACO) technique. ACO is a technique used to solve complex optimization problems and is inspired from the behavior of groups or swarming insects [8, 9]. ACO has been employed in various control applications such as optimizing the proportional-integral-derivative (PID) control parameters [10].

Optimal tuning of control parameters guarantees effective performance of the control system in a wide operational range if a proper objective function for the investigated system such as minimizing the integral time absolute error (ITAE) is developed [11]. In this paper the control parameters of the proposed SMES-CES-PSS damping scheme are simultaneously tuned using the ACO technique. Robustness of the proposed scheme is tested on a single machine infinite bus (SMIB) system [12].

II. SYSTEM MODELING

In this section, the block diagram models of the SMIB and the proposed damping scheme are briefly elaborated.

A. SMIB Model

The SMIB system comprises a synchronous generator that can be modeled as shown in Fig. 1. In this model the main input parameter is the mechanical torque ΔT_m while the rotor angle $\Delta\delta$ is the main output parameter. The entire model of the SMIB with all sub-models for the governor, steam turbine and excitation system is shown in Fig. 2. More details about this model can be found in .

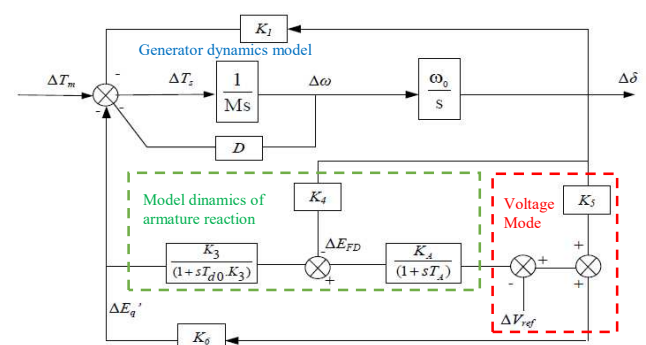


Fig. 1. Synchronous machine block model.

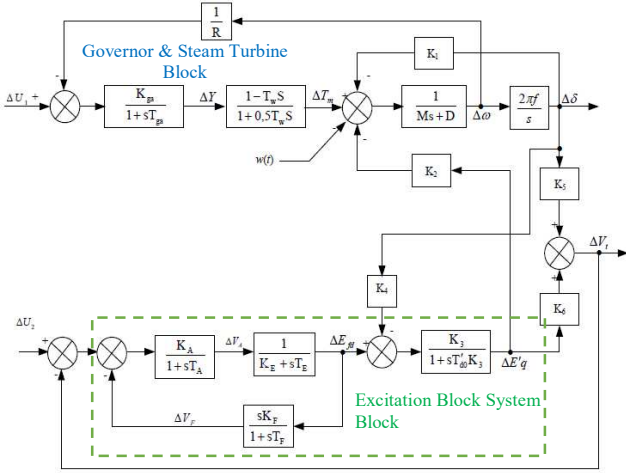


Fig. 2. Block Model of SMIB.

B. Modeling of PSS, SMES and CES

PSS is normally used to maintain the stability of a power system, the model for PSS is as shown in Fig. 3. The model consists of cascaded first order blocks with specific time constants as detailed in [13].

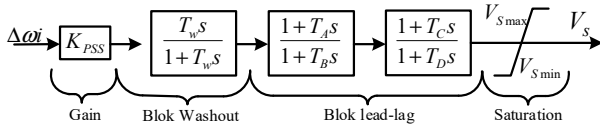


Fig. 3. PSS Block Model.

SMES stores energy in a magnetic field created by the DC current flowing through a superconducting coil which is cooled by a cryogenic system. The SMES coil could be of low temperature, cooled by liquid Helium or high temperature, cooled by liquid Nitrogen [14]. A recent technology has achieved superconductivity state at room temperature and is expected to revolutionize and advance the application of superconductors in power systems. The superconductor is interfaced to the power system by a power conditioning system (PCS) to control the energy exchange among them. Based on the operating condition of the power system, the SMES system has three operational modes; charging, standby and discharging [9]. Equations (1) through (5) are used for modeling the SMES.

$$V_{SM} = D * V_{DC} \quad (1)$$

$$-V_{SM} = (1 - D) * V_{DC} \quad (2)$$

$$I_{SM} = \frac{1}{L_{SM}} \int_{t_0}^t V_{DC} d\tau + I_{SM0} \quad (3)$$

$$P_{SM} = V_{SM} I_{SM} \quad (4)$$

$$W_{SM} = \frac{1}{2} L_{SM} I_{SM}^2 \quad (5)$$

Equation (1) is applied during SMES charging mode, where V_{SM} is the voltage across the SMES coil, V_{DC} is the voltage across the DC link capacitor of the PCS and D is the duty cycle. Equation (2) is applicable during the SMES discharging mode while (3) correlates the SMES current I_{SM} with the SMES voltage; I_{SM0} is the initial conductor current. Equation (4) is the power P_{SM} that can be modulated by the coil

and (5) is the energy stored in the SMES coil. To increase system damping, the SMES is connected at the terminal of the generator. The SMES configuration including a PID controller can be represented by the diagram shown in Fig. 4 [9, 10].

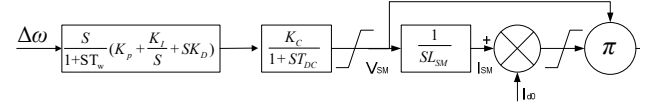


Fig. 4. SMES Block Model

The CES consists of a storage capacitor and a power conversion system with a typical configuration as shown in the block diagram of Fig. 5 [15].

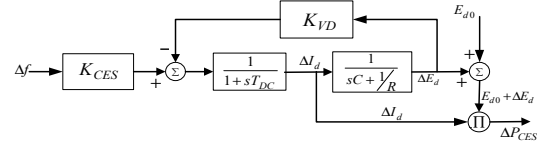


Fig. 5. CES Block Model

The applied formulas for CES are listed below:

$$E_d = 2E_{d0} \cos\alpha - 2I_d R_D \quad (6)$$

$$E_{d0} = \frac{[E_{dmax}^2 + E_{dmin}^2]^{1/2}}{2} \quad (7)$$

Where E_d is the capacitor voltage with initial value of E_{d0} and minimum / maximum values of E_{dmin} , E_{dmax} ; respectively. R_D and α are respectively the Resistor Energy Dissipation and Phase Angle. If a fault occurs while the capacitor voltage is too low, the energy required by the system may intermit the control mechanism. To solve this problem, 30% of the capacitor low voltage limit (E_{d0}) is applied.

$$E_{dmin} = 0.3E_{d0} \quad (8)$$

After fault, the nominal CES voltage should retain its initial value. To allow quick voltage recovery, the capacitor voltage deviation ΔE_d is used as a negative feedback signal in the CES control loop which is calculated from:

$$\Delta E_d = \left[\frac{1}{sC + 1/R} \right] \Delta I_d \quad (9)$$

The CES Output Power transferred to the system is:

$$\Delta P_{CES} = (E_{d0} + \Delta E_d) \cdot \Delta I_d \quad (10)$$

C. Ant Colony Optimization

The ant selects a path from point r to point s on a journey with a probability $p(r, s)$ calculated from:

$$p(r, s) = \frac{\gamma(r, s)}{\sum_t \gamma(r, t)} s, l \in N_r^k \quad (11)$$

where the matrix $\gamma(r, s)$ is the amount of pheromone intensity between points r and s .

Then the pheromones are updated using the below equation.

$$\gamma(r, s) = \alpha \cdot \gamma(r, s) + \Delta y^k(r, s) \quad (12)$$

where α , in the range $0 < \alpha < 1$, represents the resistance of a pheromone, then $(1 - \alpha)$ represents the evaporation that occurs in pheromones and $\Delta y^k(r, s)$ is the number of pheromones that ants k drop on the path (r, s) .

The pheromone trail (r, s) for the best trip made by the ants is updated using (13).

$$\gamma(r, s) = \alpha \cdot \gamma(r, s) + \frac{Q}{f_{\text{best}}} r, s \in J_{\text{best}}^k \quad (13)$$

where Q is a very large positive constant.

In order to avoid a situation where the ants following the same path, which results in the same solution, the strength of the pheromone trail is limited to the following intervals:

$$\gamma(r, s) = \begin{cases} \tau_{\min} & \text{if } \gamma(r, s) \leq \tau_{\min} \\ \tau_{\max} & \text{if } \gamma(r, s) \geq \tau_{\max} \end{cases} \quad (14)$$

The solution of the ant colony journey in the optimization of PSS-SMES-CES control parameters is plotted into a graph to the maximum iteration limit.

Integral Time Absolute Error (ITAE) as given by (15) is used as the objective function to improve system stability during load dynamic changes.

$$ITAE = \int_0^t |\Delta f(t)| dt \quad (15)$$

where Δf and t are the Change of Frequency and time; respectively.

Parameters used for the proposed ACO are listed in Table I. The tuned control parameters for PSS-SMES-CES obtained by the ACO are: T_{dc} , K_{smes} , K_{pss} , T_1 , T_2 , T_3 , T_4 , T_{dc} , and K_{DE} along with the minimum and maximum limits for each parameter are shown in Table II.

| Parameters | Values |
|-------------------|--------|
| Number of Ants | 9 |
| Maximum Iteration | 50 |
| Pheromone (Alpha) | 0.9 |
| Beta | 2 |

Fig. 4 shows the convergence characteristic of the optimization process to tune the parameters of the PSS-SMES-CES using ant colony. It can be seen that the ACO does not require a long time to carry out the optimization process and it reaches a least minimum value of $6.183e-08$ for the objective function at the 30th iteration.

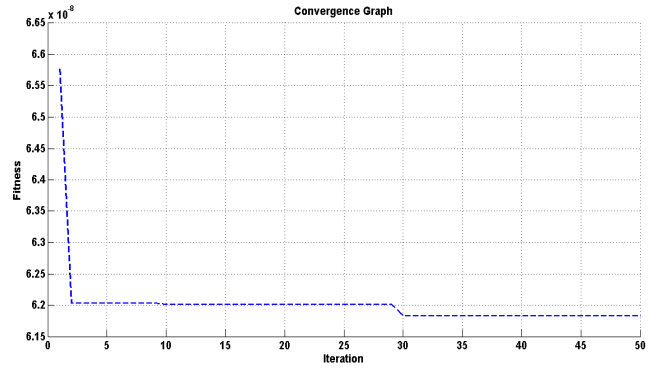


Fig. 4. ACO convergence characteristic.

TABLE II. LIMITS AND ACO OPTIMIZATION RESULTS

| Parameter | Limits | | Results |
|------------|--------|-------|----------|
| | Lower | Upper | |
| T_{dc} | 0 | 11 | 0.0267 |
| K_{smes} | 0 | 200 | 197.7554 |
| K_{pss} | 0 | 70 | 64.4572 |
| T_1 | 0 | 1 | 0.0506 |
| T_2 | 0 | 1 | 0.0380 |
| T_3 | 0 | 1 | 1.18 |
| T_4 | 0 | 1 | 5.4524 |
| T_{dcl} | 0 | 1 | 0.0512 |
| K_{de} | 0 | 100 | 85.1778 |

III. SIMULATION RESULTS AND DISCUSSION

In this paper, system performance is assessed through the investigation of the system frequency response and generator rotor angle profile using MATLAB/Simulink. The analysis is carried out with different control method options including uncontrolled SMIB, SMIB-PSS, SMIB-SMES, SMIB-CES, SMIB-SMES-CES and SMIB-SMES-CES-PSS under dynamic load changes.

A. Frequency Response of SMIB

Fig. 5 shows the simulation results of the SMIB frequency response with several control options by assuming a load change of +0.01 pu at the first second followed by a load shedding of 0.005 pu at $t = 20$ s. In the first load change, there is an increase in load, which causes imbalance between the demand power (P_e) and the mechanical power (P_m), therefore, the rotor shaft speed ($\Delta\omega$) accelerates to compensate for this imbalance and the electric frequency (Δf) oscillates accordingly. If no adequate damping scheme is adopted, the machine may become out of synchronism, causing system instability. A proper damping control system is essential to suppress system oscillations and retain the system steady state conditions. It can be observed from Fig. 5 that, even with such slight load change, the system will exhibit overshooting and relatively long time to settle down if no controller is adopted. The numerical values of the maximum overshooting of the frequency response subject to a 0.01 increment in the load for different control options are listed in Table III. Results in Fig. 5 and Table III show that the SMIB system without control exhibits a frequency overshooting in the range -0.0002408 to 0.000186 pu. This range is significantly reducing by employing one of the control approaches proposed above with a best performance achieved when the SMES-CES-PSS hybrid scheme is used.

When the load is reduced at $t=20$ s, the electrical power (P_e) becomes less than the mechanical power (P_m). This condition also causes fluctuation in the rotor speed and the electric frequency (Δf) which goes upward before returning back to steady state. The characteristics of the overshooting response in this condition are listed in Table IV.

From Fig. 5 and Table IV, it can also be observed that the proposed combined scheme comprising SMES-CES-PSS provides the best damping performance in terms of the maximum overshooting and settling time reduction.

TABLE III. FREQUENCY DEVIATION DURING LOAD INCREMENT

| Deviation | Overshoot (pu) |
|-------------------|------------------------|
| SMIB (without) | -0.0002408 & 0.000186 |
| SMIB-PSS | -0.0001937 & 6.278e-05 |
| SMIB-SMES | -0.0001445 & 1e-05 |
| SMIB-CES | -0.0001367 & 3.54e-06 |
| SMIB-SMES-CES | -0.0001361 & 3.185e-06 |
| SMIB-SMES-CES-PSS | -9.772e-05 & 9.258e-07 |

TABLE IV. FREQUENCY DEVIATION DURING LOAD SHEDDING

| Deviation | Overshoot (pu) |
|-------------------|------------------------|
| SMIB(without) | -9.361e-05 & 0.0001195 |
| SMIB-PSS | -3.439e-05 & 9.713e-05 |
| SMIB-SMES | -2.535e-06 & 7.085e-05 |
| SMIB-CES | -1.569e-06 & 6.764e-05 |
| SMIB-SMES-CES | -1.379e-06 & 6.731e-05 |
| SMIB-SMES-CES-PSS | -5.202e-07 & 4.843e-05 |

B. Rotor Angle Response

Rotor angle response to a load change of $+0.05$ pu at $t=1$ s is investigated without and with various control options. As can be seen in Fig. 5 and Table V, the rotor angle decrease from the initial condition with significant oscillations if no control scheme is used. This may result in system instability.

TABLE V. ROTOR ANGLE DEVIATION DURING LOAD INCREMENT

| Deviation | Overshoot (pu) |
|-------------------|----------------|
| SMIB(without) | -0.03667 |
| SMIB-PSS | -0.02418 |
| SMIB-SMES | -0.02391 |
| SMIB-CES | -0.0218 |
| SMIB-SMES-CES | -0.022 |
| SMIB-SMES-CES-PSS | -0.02176 |

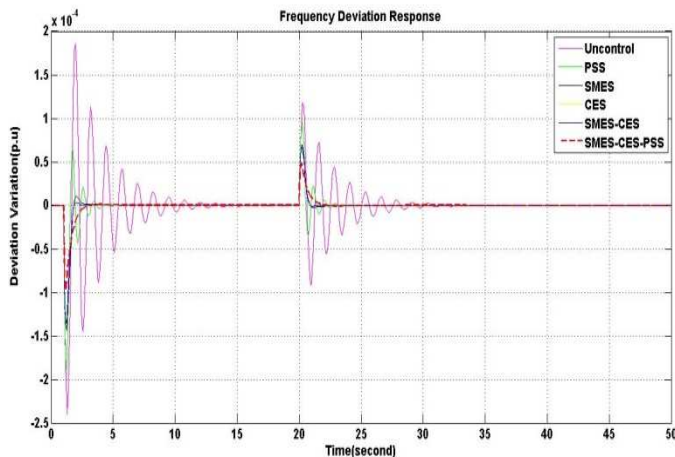


Fig. 5. Frequency Response of SMIB

Table V shows the reduction in the maximum overshooting when a damping control scheme is utilized. The proposed method using PSS-SMES-CES resulted in the smallest overshooting of -0.01762 pu with a settling time of 4.268 s.

Similar to the above scenario, the system performance is also investigated under a load reduction at $t = 20$ s. In this case, the response of the rotor angle increases from the initial stable condition before the disturbance with substantial oscillations as can be seen in Fig. 6 and Table VI. This occurs due to the magnetic coupling that pushes the stator field with the rotor field, so that the rotor angle of the generator increases. Table VI indicates that the smallest overshooting, 0.01104 pu with a settling time of 24.91 s is attained by employing the proposed SMES-CES- PSS system.

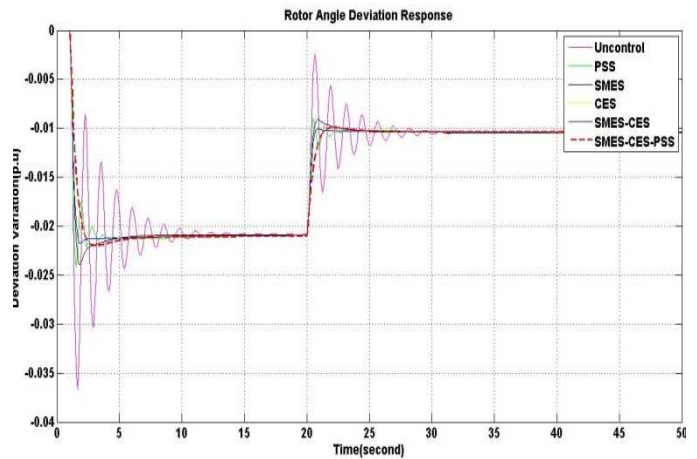


Fig. 6. Rotor Angle Response of SMIB

TABLE VI. ROTOR ANGLE DEVIATION DURING LOAD SHEDDING

| Deviation | Overshoot (pu) |
|-------------------|----------------|
| SMIB(without) | 0.01808 |
| SMIB-PSS | 0.01204 |
| SMIB-SMES | 0.01173 |
| SMIB-CES | 0.01087 |
| SMIB-SMES-CES | 0.01104 |
| SMIB-SMES-CES-PSS | 0.01084 |

The application of PSS and Energy Storage based on SMES and CES can improve the performance of the SMIB system with optimal parameters, this is indicated by an analysis of the optimal system overshoot and rotor angle. This increase in performance has an impact on the system so that the operation of the electric power system will be more optimal.

IV. CONCLUSION

Power systems are subjected to frequent load changes. This dynamic load change is expected to increase with the increase of renewable energy sources of intermittent characteristics into the grids. The conventional PSS may not be effective damping scheme in this case and additional controllers must be adopted to maintain system stability. Results obtained in this paper indicate that even with a slight load variation, system frequency and rotor angle will exhibit oscillations that if not properly damped, system instability may take place. The use of storage technology such as SMES and CES

is very promising in overcoming this issue. However, for optimum performance and with the expected significant variation of the loads in the future grids, a combination of SMES-CES-PSS is recommended. While the cost of SMES technology may be relatively high, the new discovery of a superconductor that can function at room temperature will make this technology affordable in the very near future. For further research, other storage combinations are proposed, such as Battery Energy Storage (BES).

V. ACKNOWLEDGEMENTS

The authors would like to thank Ministry of Education, Culture, Research and Technology, director general of higher education, Director of Resources of Education, Culture, Research and Technology and Center for Research and Community Service State Polytechnic of Ujung Pandang for supporting the Research.

REFERENCES

- [1] J. J. Jamani, Z. A. A. Mohd, S. Makmur, M. W. Mustafa, and H. Mokhlis, "A novel TVA-REPSO technique in solving generators sizing problems for south sulawesi network," *Przegląd Elektrotechniczny*, vol. 89, no. 2A, pp. 170-174, 2013.
- [2] M. Y. Yunus, M. R. Djalal, and Marhatang, "Optimal Design Power System Stabilizer Using Firefly Algorithm in Interconnected 150 kV Sulsebar System, Indonesia," *International Review of Electrical Engineering (IREE)*, vol. 12, no. 3, pp. 250-259, 2017.
- [3] M. R. Djalal, A. Imran, and I. Robandi, "Optimal placement and tuning power system stabilizer using Participation Factor and Imperialist Competitive Algorithm in 150 kV South of Sulawesi system," in *Intelligent Technology and Its Applications (ISITIA), 2015 International Seminar on*, 2015, pp. 147-152: IEEE.
- [4] M. R. Djalal, H. Setiadi, D. Lastomo, and M. Y. Yunus, "Modal Analysis and Stability Enhancement of 150 kV Sulsebar Electrical System using PSS and RFB based on Cuckoo Search Algorithm," *International Journal on Electrical Engineering and Informatics*, vol. 9, no. 4, pp. 800-812, 2017.
- [5] T. Bixiang, M. L. McAnelly, and G. Guoxiang, "Experimental parameter tuning of power system stabilizer," in *2012 24th Chinese Control and Decision Conference (CCDC)*, 2012, pp. 2132-2137.
- [6] D. Guha, P. K. Roy, and S. Banerjee, "Optimal Design of Superconducting Magnetic Energy Storage Based Multi-area Hydro-Thermal System Using Biogeography Based Optimization," in *2014 Fourth International Conference of Emerging Applications of Information Technology*, 2014, pp. 52-57.
- [7] M. Ponnusamy, B. Basavaraja, and S. Dash, "Load Frequency Control of Multi Area SSSC and CES Based System Under Deregulation Using Particle Swarm Optimization," *International Review of Electrical Engineering (IREE)*, vol. 10, 02/28 2015.
- [8] W. N. Chen, D. Z. Tan, Q. Yang, T. Gu, and J. Zhang, "Ant Colony Optimization for the Control of Pollutant Spreading on Social Networks," *IEEE Transactions on Cybernetics*, vol. 50, no. 9, pp. 4053-4065, 2020.
- [9] T. Huang, W. Lin, C. Xiong, R. Pan, and J. Huang, "An Ant Colony Optimization-Based Multiobjective Service Replicas Placement Strategy for Fog Computing," *IEEE Transactions on Cybernetics*, pp. 1-14, 2020.
- [10] S. Qiu *et al.*, "Ant Colony Optimization Tuning PID Algorithm for Precision Control of Functional Electrical Stimulation," *Biomedical Engineering/Biomedizinische Technik*, 2013.
- [11] A. Ala Eldin Abdallah and R. B. Mamat, "Refine PID tuning rule using ITAE criteria," in *2010 The 2nd International Conference on Computer and Automation Engineering (ICCAE)*, 2010, vol. 5, pp. 171-176.
- [12] B. Baadji, H. Bentarzi, and A. Bouaoud, "SMIB power system model with PSS for transient stability studies," in *2017 5th International Conference on Electrical Engineering - Boumerdes (ICEE-B)*, 2017, pp. 1-5.
- [13] R. Kelvianto, H. Setiadi, and I. Robandi, *Desain Analog Prototype Model of Static Synchronous Compensator (STATCOM) Pada Single Machine Infinite Bus (SMIB) Menggunakan Deferential Evolution (DE)*. 2013.
- [14] H. Setiadi and K. Jones, "Power System Design using Firefly Algorithm for Dynamic Stability Enhancement," *Indonesian Journal of Electrical Engineering and Computer Science*, vol. 1, p. 446, 03/01 2016.
- [15] R. Wijanarko, H. Setiadi, and T. Nugroho, "Coordination of SPS and CES to Mitigate Oscillatory Condition on Power Systems," *Telkonnika (Telecommunication Computing Electronics and Control)*, vol. 15, pp. 1601-1609, 12/01 2017.